ACS Sustainable Chemistry & Engineering

Research Article

Cite This: ACS Sustainable Chem. Eng. 2019, 7, 16549−16559

pubs.acs.org/journal/ascecg

Altering Extracellular Biopolymers and Water Distribution of Waste Activated Sludge by Fe(II) Persulfate Oxidation with Natural Zeolite and Polyelectrolyte as Skeleton Builders for Positive Feedbacks to Dewaterability

Jianhui Wang,[†] Yujie Tan,[†] Yang Pan,[†] Guangyin Zhen,*[,†,‡] Xueqin Lu,*[,†,§] Yu Song,[∥] Youcai Zhao,[⊥] and Uthira Krishnan Ushani[#]

[†]Shanghai Key Lab for Urban Ecological Processes and Eco-Restoration, School of Ecological and Environmental Sciences, East China Normal University, Shanghai 200241, PR China

[‡]Shanghai Institute of Pollution Control and Ecological Security, 1515 North Zhongshan Road (No. 2), Shanghai 200092, PR China

[§]Institute of Eco-Chongming (IEC), 3663 N. Zhongshan Road, Shanghai 200062, PR China

[∥]Shanghai Techase Environment Protection Co., Ltd., Shanghai 200092, PR China

[⊥]The State Key Laboratory of Pollution Control and Resource Reuse, School of Environmental Science and Engineering, Tongji University, Shanghai 200092, PR China

[#]Department of Biotechnology, Karpagam Academy of Higher Education, Coimbatore 641021, India

Supporting Information

ABSTRACT: Ferrous persulfate ($Fe(II)/S_2O_8^{2-}$) oxidation has gained much attention due to its outstanding oxidizability and high efficiency in upgrading waste activated sludge (WAS) dewaterability. Even though the $Fe(II)/S_2O_8^{2-}$ technique possesses a myriad of advantages, its potential could be further magnified for future upscaling and real-world application especially when coupled with other alternative chemicals. In this study, the potential benefits of $Fe(II)/S_2O_8^{2-}$ oxidation coupled with natural zeolite and poly(dimethyl diallyl ammonium chloride) (PDADMAC) for enhancing WAS dewaterability were investigated. The vacuum filtration test was used to evaluate the dewatering effectiveness. Variations in different extracellular polymeric substance (EPS) fractions, water distribution, functional groups, and microstructures were identified to elucidate the underlying dewatering principles and kinetics. The results demonstrated that the combination of $Fe(II)/S_2O_8^{2-}$ with zeolite and PDADMAC had a significant effect on enhancing WAS dewaterability. The optimal conditions obtained were 2.25/1.8 mmol-$Fe(II)/S_2O_8^{2-}$/g-VS, 0.5 g-zeolites/g-VS, and 0.3 g-PDADMAC/g-VS with up to 117 g-H_2O/g-VS removal (moisture content: 64.5%). Further analysis revealed the three-step dewatering mechanisms: (i) the $SO_4^{\cdot-}$ generated by $Fe(II)/S_2O_8^{2-}$ oxidation attacked the WAS flocs and cells, broke the bonds of O−H, C−C, and O═C—NH− in high-molecular-weight biopolymers, and decomposed them into micromolecule organics and even inorganics, thus liberating EPS- and cell-bound water, (ii) the broken WAS flocs were then reflocculated via adsorption bridging and charge neutralization induced by PDADMAC, and (iii) during the subsequent filtration, zeolites created channels/cavities for water release by forming a multiple void skeletal lattice while alleviating the clogging of filtration cloth. In addition, the cost-benefit analysis revealed that the combined $Fe(II)/S_2O_8^{2-}$/zeolites/PDADMAC process represented much greater attractiveness in saving cost and real implementations than the zerovalent iron/persulfate and classical Fenton process.

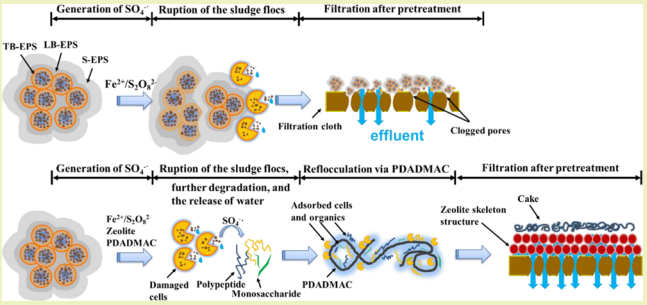

KEYWORDS: *waste activated sludge, dewaterability, $Fe(II)/S_2O_8^{2-}$ oxidation, zeolites, poly(dimethyl diallyl ammonium chloride)*

INTRODUCTION

Waste activated sludge (WAS), as the main byproduct originated from daily wastewater treatment, contains many toxic substances including heavy metals, pathogens, and high organics. However, most of them are not treated and disposed properly.[1] Dewatering plays a significant role in the transportation and disposal of the WAS, which is closely related to the cost of the subsequent treatment.[2] Raw WAS has difficulties to dewater due to its colloidal[3] and porous fractal network structure,[4] making it a challengeable issue.

Received: July 5, 2019
Revised: July 28, 2019
Published: August 30, 2019

Downloaded via MACQUARIE UNIV on July 18, 2020 at 09:20:08 (UTC).
See https://pubs.acs.org/sharingguidelines for options on how to legitimately share published articles.

 © 2019 American Chemical Society

DOI: 10.1021/acssuschemeng.9b03842
ACS Sustainable Chem. Eng. 2019, 7, 16549−16559

Table 1. Physicochemical Properties of Waste Activated Sludge Used in This Study[a]

moisture content (wt %)	pH	TS (mg/L)	VS (mg/L)	CST (s)	TCOD (g/L)	SCOD (mg/L)	protein (mg/g-VS)	polysaccharide (mg/g-VS)
98.3 ± 1.00.01	6.8 ± 0.1	16.7 ± 0.4	6.2 ± 0.2	386.6 ± 11.4	18.2 ± 0.8	1031.8 ± 10.1	38.7 ± 2.0	30.6 ± 1.0

[a]TCOD: total chemical oxygen demand; SCOD: soluble chemical oxygen demand; TS: total solids; VS: volatile solids; CST: capillary suction time.

There have been numerous methods available in the literature to enhance the dewaterability, including microwave,[5] acid,[6] ultrasound,[7] electrochemical process,[8] and advanced oxidation such as Fenton reagent, and Fe(II)/$S_2O_8^{2-}$ oxidation.[9] Among them, Fe(II)/$S_2O_8^{2-}$ oxidation has showed the great promise for strengthening WAS dewaterability. Powerful $SO_4^{\cdot -}$ can be generated when potassium persulfate reacts with ferrous sulfate heptahydrate, which degrades the organic compounds and disintegrates the WAS flocs. Zhen et al.[9] intiated the phenomenon of 88.8% capillary suction time (CST) reduction within 1 min in the presence of 1.5 mmol-Fe(II)/g-VSS and 1.2 mmol-$S_2O_8^{2-}$/g-VSS. Additionally, differing from the single Fe(II)/$S_2O_8^{2-}$ oxidation process, Zhen et al.[10,11] reported that Fe(II)/$S_2O_8^{2-}$ oxidation combined with the electrolysis or microwave irradiation process could more profoundly enhance the WAS dewaterability. Even though the methods mentioned above possess a lot of advantages including low-level residual, cost saving, and strong oxidation,[9−11] the potential of the Fe(II)/$S_2O_8^{2-}$ technique could be further improved for future upscaling and real-world application if combined with other alternative processes.

Chemical conditioning methods are often applied to condition and disintegrate WAS flocs, with the purpose of promoting some specific physicochemical properties (e.g., solid solubilization, dewaterability, etc.). However, a lot of oxidation methods had very limited benefits on and even deteriorated the WAS settleability against the ultimate disposal. A previous work by Wu et al.[12] observed that K_2FeO_4 oxidation deteriorated WAS settleability, while the results documented in the WAS conditioning by utilizing the Fe(II)/$S_2O_8^{2-}$ technique[13] show that such a method possesses the extraordinary capability of enhancing the dewatering process. However, an issue faced by the Fe(II)/$S_2O_8^{2-}$ technique is the disintegration of WAS flocs and particle size reduction caused by $SO_4^{\cdot -}$ oxidation, which induces filter cloth clogging when subjected to the filter press. One alternative strategy to alleviate such a technical problem can be the combination with polyelectrolytes. Polyelectrolytes especially cationic polyelectrolytes are able to enhance the liquid−solid separation of WAS on account of the electrostatic attraction between the floc surfaces and cationic polyelectrolyte.[14] Poly(dimethyl diallyl ammonium chloride) (PDADMAC) is one of the strong cationic polyelectrolytes, which is usually used to improve flocculation of particles in wastewater treatment. A previous research coupling PDADMAC with Fe_2O_3 and H_2SO_4 has revealed the potential of PDADMAC in promoting WAS dewatering.[15] In this regard, an appropriate addition of PDADMAC might exert a positive effect on enhancing Fe(II)/$S_2O_8^{2-}$ oxidation performance in WAS dewatering.

Another issue is the rapid formation of the WAS cake layer in the close vicinity of the filter medium during the mechanical dewatering in practice, the presence of which will block pores of filter cloth, ultimately causing the diminution of the water flow rate. Physical conditioners, generally known as skeleton builders or filter aids, are widely used to slow down the compression rate of WAS and enhance the subsequent permeability via forming permeable and more rigid lattice structures.[16] Up to now, numerous carbon-based materials have been employed as physical conditioners, including char, coal fines, organic waste,[17] and lignite.[16]

Zeolites are crystalline microporous aluminosilicates, containing corner-sharing SiO_4^- and AlO_4^- tetrahedra,[18,19] and adjacent tetrahedra are linked at the corners via a common oxygen atom.[20] Zeolites have been widely utilized as an adsorbent[21,22] and catalyst in wastewater purification and contamination removal (e.g., ammonia nitrogen).[23] Also, natural zeolite particles have been demonstrated to have the ability of enhancing the filterability by acting as a skeletal builder during filtration.[16] Therefore, the joint use of zeolites will further stimulate the dewatering performance of Fe(II)/$S_2O_8^{2-}$. For instance, more efficient *p*-chlorophenol degradation was reported when combining Fenton oxidation with Fe-containing ZSM-5 zeolite.[24] However, the research on coupling Fe(II)/$S_2O_8^{2-}$ with zeolites and PDADMAC for WAS dewaterability is still unavailable in the literature.

Therefore, the specific objective of this research was to evaluate the potential of combined Fe(II)/$S_2O_8^{2-}$, zeolites, and PDADMAC as an innovative technique for enhancing WAS dewaterability. The water removal rate during the mechanical filtration process was recorded and used as the main indicator of dewaterability. To gain a comprehensive investigation into the dewatering principles, the drying test and differential scanning calorimetry (DSC) were performed and different EPS fractions were extracted to reveal their respective role in sludge dewatering. A confocal laser scanning microscope (CLSM) was used to visualize the spatial distribution of bacteria cells and biopolymers in the sludge flocs. Furthermore, X-ray photoelectron spectroscopy (XPS) and scanning electron microscopy integrating energy-dispersive X-ray spectrometry (SEM-EDS) were conducted to characterize the variations in functional groups and the microstructure of WAS under different conditions to reveal the underlying dewatering kinetics. Finally, a desktop scalingup cost-benefit analysis was carried out to explore the practice potential of the Fe(II)/$S_2O_8^{2-}$/zeolites/PDADMAC process.

■ METHODS AND MATERIALS

Experimental Materials. WAS used in this study was collected from a secondary clarifier of a wastewater treatment plant (WWTP) in Shanghai, China. The collected sample was transferred to the laboratory within 2 h and stored at 4 °C. All the related experiments were completed within 48 h after sampling. The physicochemical properties of the WAS are listed in Table 1. Potassium persulfate ($K_2S_2O_8$, >99.5%), ferrous sulfate heptahydrate ($FeSO_4{\cdot}7H_2O$, >99.0%), zeolites (66.5% SiO_2, 12.30% Al_2O_3, 150 μm), and PDADMAC (M_w 400,000−500,000, 20 wt %, 800−1000 cP, 25 °C) were purchased from Sinopharm Chemical Reagent Co., Ltd. (Shanghai, China). All the chemical reagents used in this investigation were prepared freshly when used.

Procedures for WAS Conditioning. A series of experiments were conducted in a 250 mL beaker with 200 mL of WAS sample at inherent pH unless requested elsewhere. The Fe(II)/$S_2O_8^{2-}$ reagent was first added into the sample, followed by zeolites and then by

DOI: 10.1021/acssuschemeng.9b03842
ACS Sustainable Chem. Eng. 2019, 7, 16549−16559

PDADMAC. During the whole process, WAS samples were continuously agitated at 300 rpm to ensure their homogeneity. The ratio of Fe(II)/$S_2O_8^{2-}$ was kept at 1.25:1.[9] The dosage of persulfate for the experiments was varied from 0.0 to 0.6, 1.2, 1.8, 2.4, 3.0, and then to 3.6 mmol/g-VS (WAS), and the corresponding dosage of Fe(II) was 0.0, 0.75, 1.5, 2.25, 3, 3.75 to 4.5 mmol/g-VS. The dosage of zeolites was 0.0, 0.075, 0.15, 0.3, 0.5, 0.65, and 0.8 g/g-VS, and the dosage of PDADMAC was 0.0, 0.15, 0.3, 0.5, and 0.8 mL/g-VS.

Dewatering Procedures. The WAS dewaterability was evaluated by using a vacuum filtration method. About 5 mL of the sample was filtered through a 0.45 μm filter paper by applying suction pressure through a vacuum pump (GM-0.33A, China). The filtration lasted for 2 min at a vacuum pressure of −0.08 MPa, the effluent of filtrate was collected continuously, and the data of flux were collected each 2 s.

Measurement of Free Water/Bound Water (FW/BW) Content. Free water (FW) and bound water (BW) contents were measured with differential scanning calorimetry (DSC).[25] The temperature of the WAS sample was initially decreased to −60 °C at a rate of 10 °C/min, assuming that all the free water in this sample was frozen. Then, the temperature was increased to 40 °C at the same rate. FW content is obtained by integrating the peak area of the endothermic curve below the baseline that represents the heat absorbed to melt the frozen free water. BW content is calculated by the difference of the FW content to the total water (TW) content via eq 1[26]

$$\mathrm{BW} = \mathrm{TW} - \Delta H/\Delta H_0 \quad (1)$$

where ΔH is the amount of energy absorbed in the WAS sample, and ΔH_0 is the standard melting heat of ice (334.7 J/g).[27]

Characterization of Morphology via SEM-EDS. SEM-EDS (S-4800, Hitachi, Japan) was used to reveal the microstructure of WAS flocs. The samples were prepared following the previous study.[13] EDS mapping was recorded with a silicon drift detector to indicate the location of each element analyzed.

Multiple Fluorescence Labeling and CLSM Observation. For CLSM observation, sludge samples were first fixed with 2.5% glutaraldehyde in phosphate buffer for 30 min. After rinsing for three times with phosphate-buffered saline (PBS), the samples were stained with SYTO 63 (20 μM, 100 μL) and then fixed by sodium bicarbonate buffer ($NaHCO_3$, 1 M, 10 μL), followed by staining with FITC solution (10 g/L, 10 μL), ConA (0.25 g/L, 10 μL), and CW (0.3 g/L, 10 μL) step by step. After each staining, the samples were incubated in the dark for 30 min and then washed three times with PBS solution to remove the extra probes.[28] After that, the samples were stored at 4 °C for CLSM observation (TCS SP8 STED 3X, Leica, Germany).

Other Analytical Methods. Total solids (TS), volatile solids (VS), water content, total chemical oxygen demand (TCOD), and soluble chemical oxygen demand (SCOD) were determined by following the standard methods.[29] The pH meter (PHS-25, China) was used to measure the pH value. CST was determined with a capillary suction timer (Type 304 M, England) equipped with a 0.535 cm inner diameter funnel and Triton CST paper (7 × 9 cm, Electronics Ltd., England). Three kinds of EPS fractions were extracted,[13] and polysaccharide (PS) and protein (PN) were determined.[30,31] X-ray photoelectron spectroscopy (XPS) measurements were carried out by an RBD upgraded PHI 5000C ESCA system (PerkinElmer) with Mg Kα radiation (h = 1253.6 eV) to identify the chemical states of C, O, N, and Si in WAS samples, and the statistical analysis was completed by using the software application XPSPEAK41.

RESULTS AND DISCUSSION

Dewatering Performance via Single Fe(II)/$S_2O_8^{2-}$ or Zeolites. The water removal rate during mechanical filtration is regarded as the main indicator of dewaterability. Effects of Fe(II)/$S_2O_8^{2-}$ and zeolite dosages on the WAS dewaterability were investigated, and the results are shown in Figure 1. Fe(II)/$S_2O_8^{2-}$ oxidation did have a positive effect on

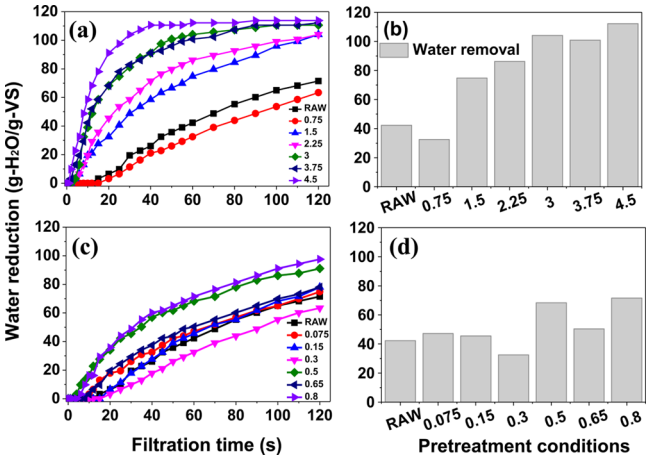

Figure 1. Variations in water removal after (a, b) single Fe(II)/$S_2O_8^{2-}$ oxidation and (c, d) single zeolites: Left, real-time water removal during filtration. Right, water removal after 60 s filtration (the Fe(II)/$S_2O_8^{2-}$ ratio was 1.25:1, and only Fe(II) dosage was presented herein).

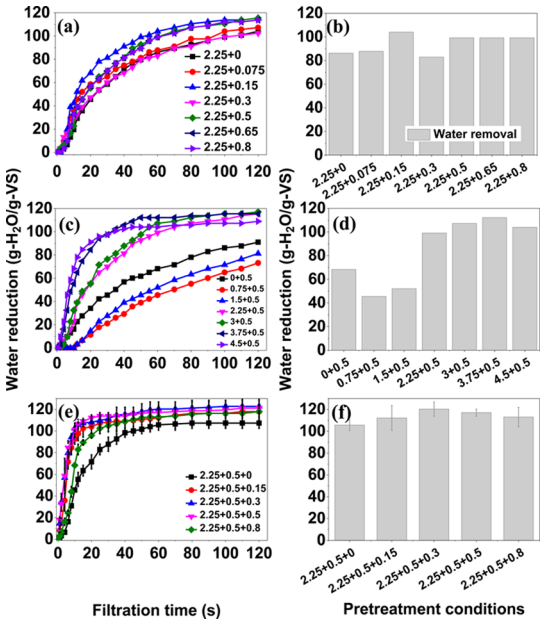

Figure 2. Variations in water removal after (a, b) fixed with zeolites, (c, d) combined with Fe(II)/$S_2O_8^{2-}$ oxidation, and (e, f) combined fixed 2.25/1.8 mmol-Fe(II)/$S_2O_8^{2-}$/g-VS oxidation and 0.5 g-zeolites/g-VS with PDADMAC: Left, real time water removal during filtration. Right, water removal after 60 s filtration (the Fe(II)/$S_2O_8^{2-}$ ratio was1.25: 1, and only Fe(II) dosage was presented herein).

enhancing WAS dewaterability (Figure S1). Water removal after 120 s filtration increased from 63.4 to 104.1 and then to 113.8 g-H_2O/g-VS as the dosage of Fe(II)/$S_2O_8^{2-}$ was increased from 0.75/0.6 to 2.25/1.8 and 3/2.4 mmol/g-VS. However, water removal was not further elevated with further increasing Fe(II)/$S_2O_8^{2-}$ dosage. In the presence of 2.25/1.8 mmol-Fe(II)/$S_2O_8^{2-}$/g-VS, water removal approached 86.2 and 104.1 g-H_2O/g-VS after 60 and 120 s of filtration, respectively (Figure 1a,b). The result matched well with our previous research studies,[9,10,32] where the fast CST reduction occurred once subjection to Fe(II)/$S_2O_8^{2-}$ oxidation. It was worth noting that after pretreatment by Fe(II)/$S_2O_8^{2-}$, water removal rose rapidly during the first 60 s and then it kept stable

DOI: 10.1021/acssuschemeng.9b03842
ACS Sustainable Chem. Eng. 2019, 7, 16549−16559

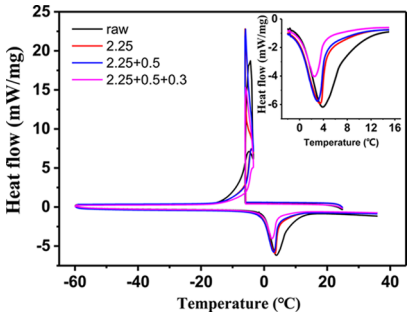

Figure 3. DSC thermograms of the raw and pretreated WAS under different conditions: raw WAS (black), 2.25/1.8 mmol-Fe(II)/$S_2O_8^{2-}$/g-VS (red), 2.25/1.8 mmol-Fe(II)/$S_2O_8^{2-}$/g-VS and 0.5 g-zeolites/g-VS (blue), and 2.25/1.8 mmol-Fe(II)/$S_2O_8^{2-}$/g-VS, 0.5 g-zeolites/g-VS, and 0.3 g-PDADMAC/g-VS (azaleine).

Table 2. Water Distribution in the Raw and Pretreated WAS Samples under Different Conditions

sample	TW (g/g-DS)	FW (g/g-DS)	BW (g/g-DS)
raw	12.35	7.84	4.51
2.25	4.09	2.63	1.46
2.25 + 0.5	3.86	2.46	1.40
2.25 + 0.5 + 0.3	3.12	1.30	1.82

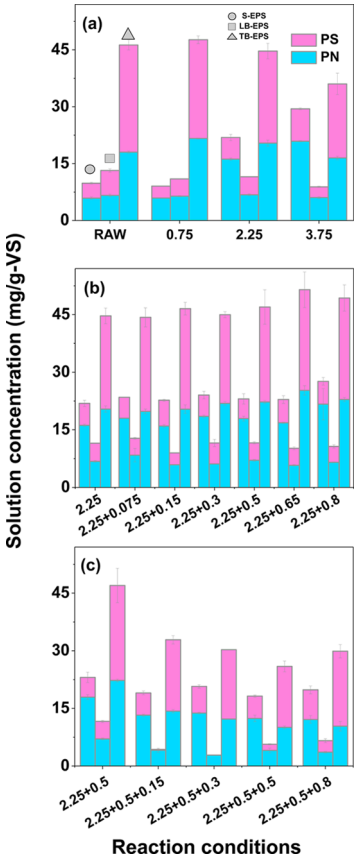

Figure 4. Variations in PN and PS contents in different EPS fractions under different conditions: (a) Fe(II)/$S_2O_8^{2-}$, (b) Fe(II)/$S_2O_8^{2-}$ and zeolites, and (c) Fe(II)/$S_2O_8^{2-}$, zeolites, and PDADMAC.

during the following 60 s. Therefore, water removal effectiveness after 60 s filtration was used for evaluating the dewaterability. As shown in Figure 1c, with the conditioning of 0.5 or 0.8 g zeolites/g-VS, WAS exhibited preferable water

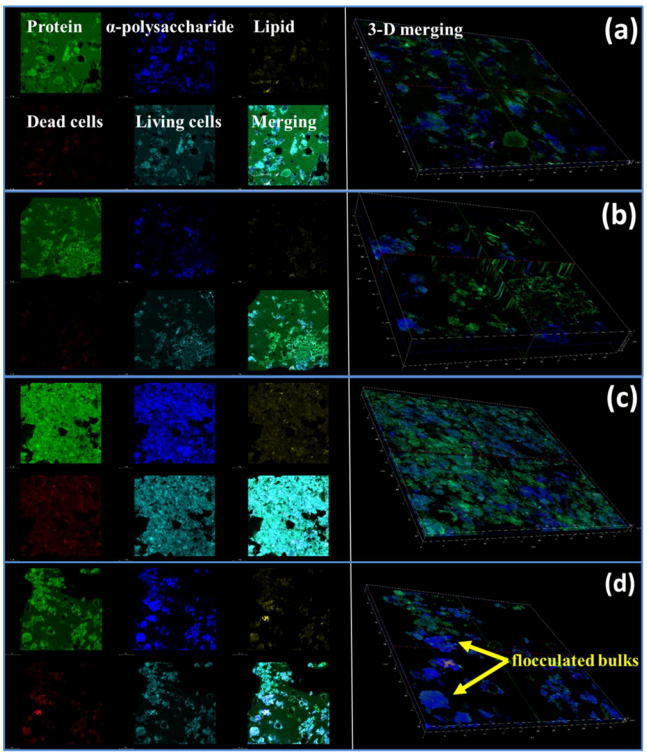

Figure 5. Variations of WAS via CLSM under different conditions: (a) raw WAS, (b) 2.25/1.8 mmol-Fe(II)/$S_2O_8^{2-}$/g-VS, (c) 2.25/1.8 mmol-Fe(II)/$S_2O_8^{2-}$/g-VS and 0.5 g-zeolites/g-VS, and (d) 2.25/1.8 mmol-Fe(II)/$S_2O_8^{2-}$/g-VS, 0.5 g-zeolites/g-VS, and 0.3 g-PDADMAC/g-VS. Left: the distribution of each component. Right: 3D distribution merging graph of all components.

removal (68.3 and 71.5 g-H_2O/g-VS, respectively, in Figure 1d and Figure S2). The particle size of WAS fell within the range of 10 to 110 μm,[11] and the particle size of zeolites used is about 150 μm. Thus, the presence of zeolites provided channels/cavities for water escaping by forming a layer of the porous medium composed of zeolites between filtration cloth and WAS flocs,[16,18,24] thus promoting the dewaterability.

Dewatering Performance via the Combined Process. When Fe(II)/$S_2O_8^{2-}$ was combined with zeolites, water removal after 60 s filtration increased apparently compared to that of the single Fe(II)/$S_2O_8^{2-}$ or zeolite pretreatment (Figure 2). Water removal reached 99.2 g-H_2O/g-VS, 15.3 and 45.2% higher than that of Fe(II)/$S_2O_8^{2-}$ and zeolites alone, respectively, especially at the dosage of 2.25/1.8 mmol-Fe(II)/$S_2O_8^{2-}$/g-VS and 0.5 g-zeolites/g-VS (Figure S3). At the fixed 0.5 g-zeolites/g-VS, water removal was elevated from 45.5 to 99.2 g-H_2O/g-VS when the Fe(II)/$S_2O_8^{2-}$ dosage was increased from 0.75/0.6 to 2.25/1.8 mmol/g-VS and then it kept stabilized even when Fe(II)/$S_2O_8^{2-}$ dosage was further increased to 4.5/3.6 mmol/g-VS (Figure 2a,b). On the other hand, during the combined process with the fixed Fe(II)/$S_2O_8^{2-}$ of 2.25/1.8 mmol/g-VS, water removal peaked (99.2 g-H_2O/g-VS) at 0.5 g-zeolites/g-VS; the further rise in zeolite dosage possessed negligible promotion on water removal (Figure 2c,d). Similarly, Liu et al.[33] found that water content of dewatered WAS cake could decrease to 49.5 ± 0.5% after pretreated by H_2O_2, Fe(II), lime, and ordinary Portland cement (OPC). This might be due to the strong oxidizing property of Fe(II)/$S_2O_8^{2-}$, which broke up the WAS flocs and released the bounded water.[9] Compared with the conventional

DOI: 10.1021/acssuschemeng.9b03842
ACS Sustainable Chem. Eng. 2019, 7, 16549−16559

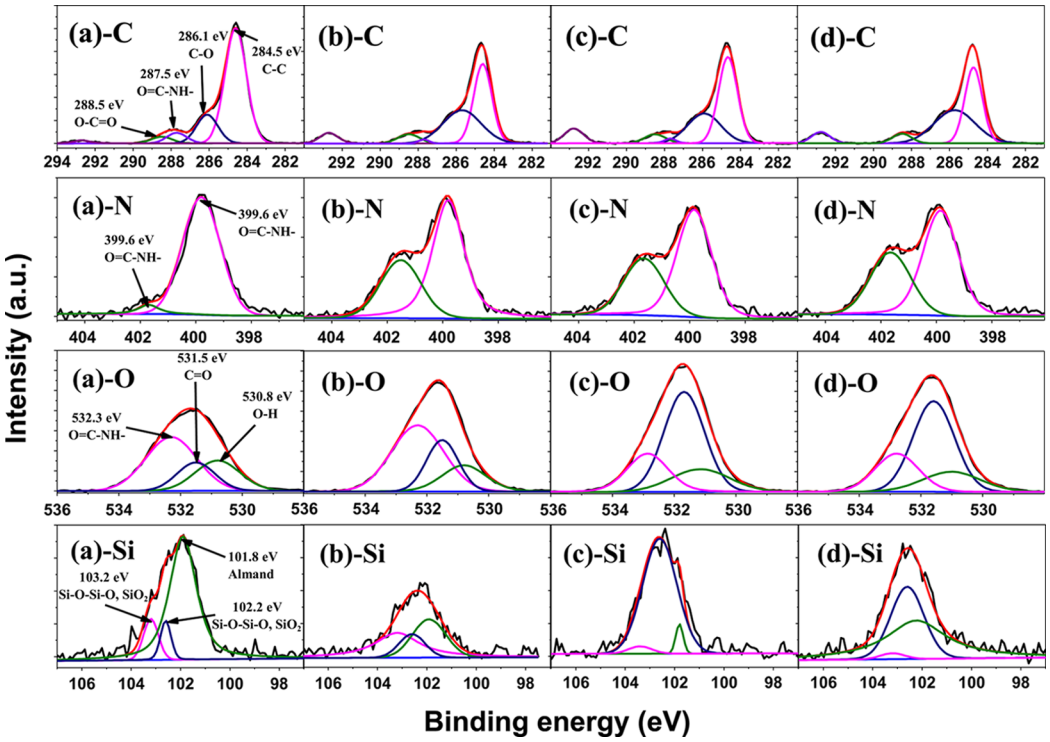

Figure 6. XPS survey scans of the WAS samples under different conditions: (a) raw WAS, (b) 2.25/1.8 mmol-Fe(II)/$S_2O_8^{2-}$/g-VS, (c) 2.25/1.8 mmol-Fe(II)/$S_2O_8^{2-}$/g-VS and 0.5 g-zeolites/g-VS, and (d) 2.25/1.8 mmol-Fe(II)/$S_2O_8^{2-}$/g-VS, 0.5 g-zeolites/g-VS, and 0.3 g-PDADMAC/g-VS.

conditioners, zeolites possess the unique advantages, including the pore widths due to the molecular dimensions and strictly uniform pore diameters.[20] In this regard, zeolites could serve as catalysts during the reaction in terms of their acid sites, offering the reaction channel and inducing more $SO_4^{\cdot -}$ generation. Meanwhile, zeolites created channels/cavities during the filtration for water release by forming a multiple void skeletal lattice, facilitating the permeation and liberation of water. As a result, the clogging of the filtrate cloth pore can be under prevention and control, and as a consequence, the dewaterability was meliorated.

PDADMAC was further combined with Fe(II)/$S_2O_8^{2-}$ and zeolites, and the results are shown in Figure 2e,f. At the fixed 2.25/1.8 mmol-Fe(II)/$S_2O_8^{2-}$/g-VS and 0.5 g-zeolites/g-VS, water removal increased from 99.2 to 117.6 g-H_2O/g-VS when PDADMAC dosage was increased from 0 to 0.3 g/g-VS, revealing the positive effect of PDADMAC on enhancing dewatering efficiency (moisture content: 64.5%) (Figure S4). PDADMAC, as a kind of high-molecular polymer, has the capability of adsorption bridging and strong charge neutralization simultaneously by means of the polymer chain. The cationic polymers colloid attracted the negatively charged WAS flocs, neutralizing the surface charge while compressing the floc diffusion layer to make the particles destabilize. As a result of this, WAS flocs were flocculated into a larger colloid, which would further enhance the effect exerted by zeolites on WAS. Furthermore, the WAS flocs can be adsorbed onto PDADMAC molecules through hydrogen bonding and van der Waals force.[34] An interesting phenomenon observed was that a slight drop (to 113.0 g-H_2O/g-VS) happened when the PDADMAC dosage was further increased to 0.8 g/g-VS. This might be attributed to the fact that the excessive PDADMAC would lead to stronger electrostatic repulsion, which hindered the floc reflocculation and thus caused the deteriorated dewaterability. The result was in line with that of Lee and Liu,[34] who reported that overdosing the polyelectrolyte increased cost and reduced WAS dewaterability. Nonetheless, in view of the abovementioned results, it is clear that the optimal conditions for WAS dewatering can be 2.25/1.8 mmol-Fe(II)/$S_2O_8^{2-}$/g-VS, 0.5 g-zeolites/g-VS, and 0.3 g-PDADMAC/g-VS. Differing from our current work, many research available in the literature did not gain satisfactory results due to long pretreatment and filtration time as well as low pH (e.g., 2 h pretreatment and 30 min filtration for Fe(III)/H_2O_2 at pH 2.0−2.5).[35] Another study reported that the moisture content of sludge cake decreased to 64.8% with the Fe@Fe_2O_3 nanomaterial, poly(diallyldimethylammonium chloride) (PDMDAAC), and H_2SO_4.[15] However, the high cost in preparing the Fe@Fe_2O_3 nanomaterial retards its real application. As a contrast, the process in this study appears much lower cost and time/energy saving due to less time required for dewatering (only 20 min for pretreatment and 2 min for filtration) and ease of operation, which is exactly the prerequisite for its practice. Similar excellent performance was found as well in the combination of zerovalent iron and hydrogen peroxide[36] and the use of free ammonia (i.e., NH_3) for improving WAS biodegradability and dewaterability.[37]

Change in Water Distribution of WAS Flocs. The water distribution of the filtrated WAS cake was analyzed through DSC to verify the role of the combined process in provoking water liberation (Figure 3). Free water (FW) and bound water (BW) contents were calculated, and the results are shown in Table 2. The peak area of the curve below the baseline radically shrank after pretreatment especially at 2.25/1.8 mmol-Fe(II)/$S_2O_8^{2-}$/g-VS, 0.5 g-zeolites/g-VS, and 0.3 g-PDADMAC/g-VS (Figure 3), which revealed that the combined process was able to efficiently remove FW. Raw WAS after 120 s filtration contained 7.84 g-FW/g-DS and 4.51

DOI: 10.1021/acssuschemeng.9b03842
ACS Sustainable Chem. Eng. 2019, 7, 16549−16559

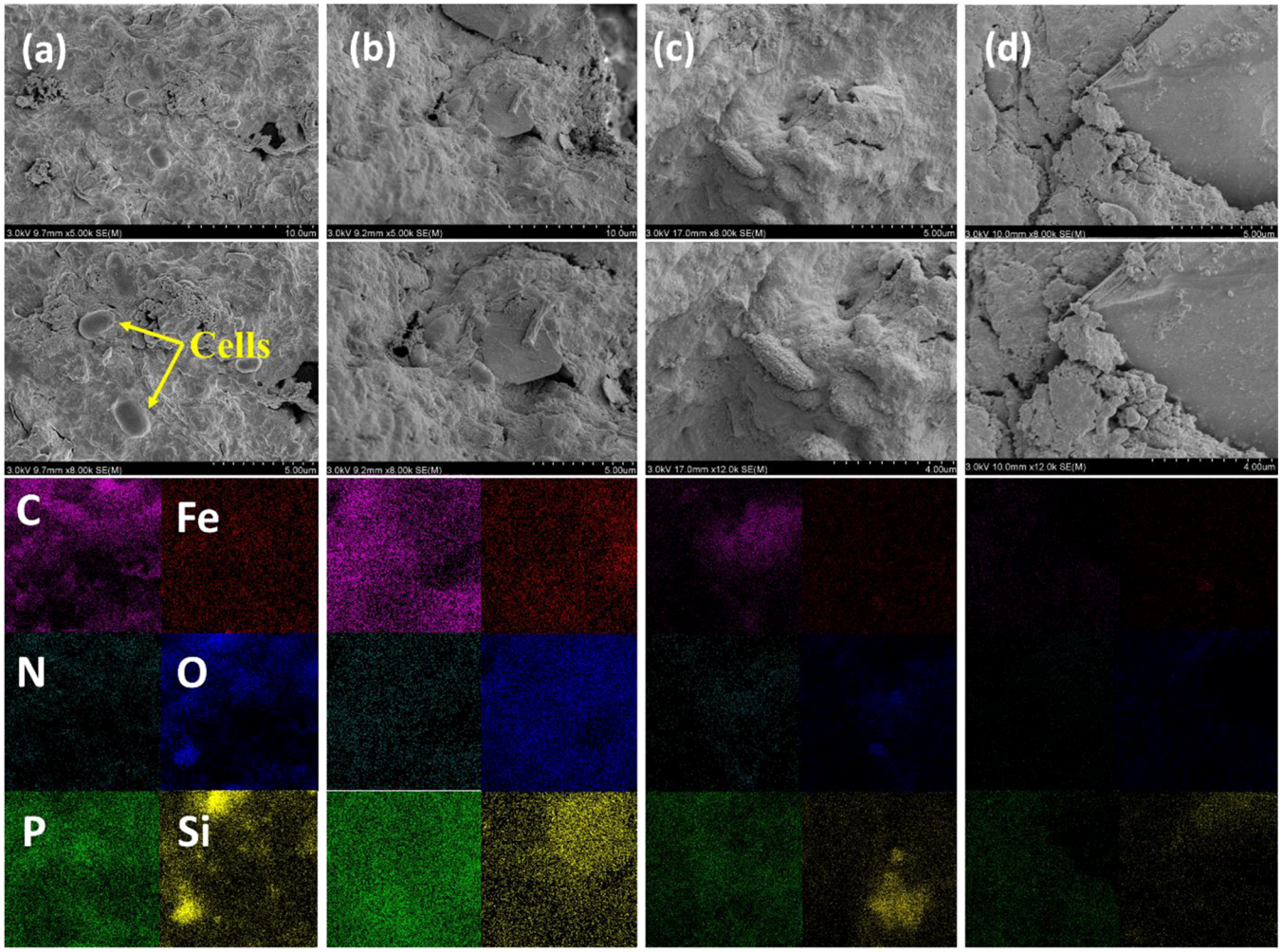

Figure 7. SEM micrographs and EPS mapping of carbon, iron, nitrogen, oxygen, phosphorus, and silicon elements of the WAS samples: (a) raw WAS, (b) 2.25/1.8 mmol-Fe(II)/$S_2O_8^{2-}$/g-VS, (c) 2.25/1.8 mmol-Fe(II)/$S_2O_8^{2-}$/g-VS and 0.5 g-zeolites/g-VS, and (d) 2.25/1.8 mmol-Fe(II)/$S_2O_8^{2-}$/g-VS, 0.5 g-zeolites/g-VS, and 0.3 g-PDADMAC/g-VS.

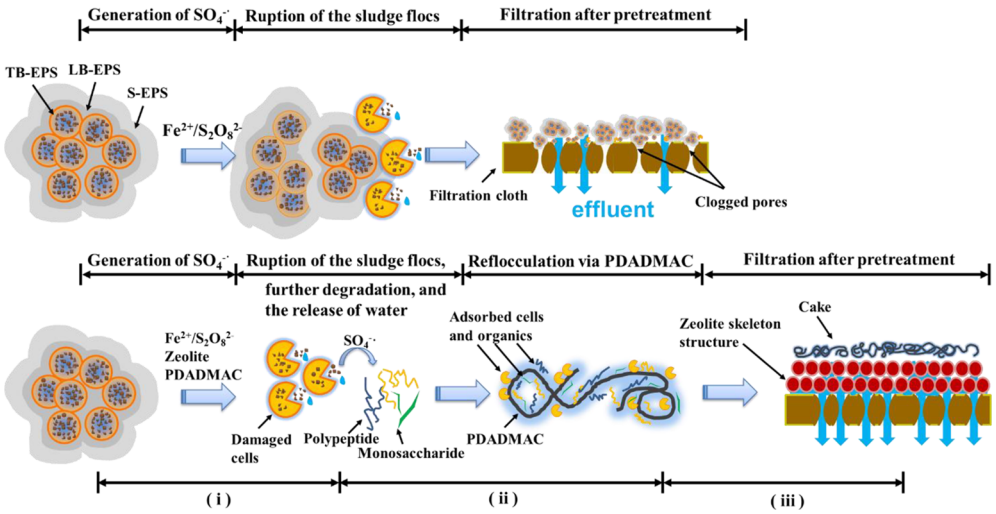

Figure 8. Possible mechanisms of promoting WAS dewatering with Fe(II)/$S_2O_8^{2-}$/zeolites/PDADMAC system.

g-BW/g-DS, and the removal behaviors of TW, FW, and BW under different conditions showed remarkable differences. As listed in Table 2, 3.05 g-BW/g-DS was transferred to FW at 2.25/1.8 mmol-Fe(II)/$S_2O_8^{2-}$/g-VS, with 66.9, 66.5, and 67.6% removal of TW, FW, and BW, respectively. It can be ascribed to the generation of $SO_4^{\cdot-}$ from Fe(II)/$S_2O_8^{2-}$oxidation, which in turn broke WAS flocs, and caused the degradation and disruption. As a result, the water bounded

DOI: 10.1021/acssuschemeng.9b03842
ACS Sustainable Chem. Eng. 2019, 7, 16549−16559

Table 3. Economic Analysis and Comparison of the Fe(II)/$S_2O_8^{2-}$/Zeolites/PDADMAC Process for WAS Dewaterability Enhancement in an Assumed WWTP with a Population Equivalent of 100,000[a]

parameters	Fe(II)/$S_2O_8^{2-}$/zeolites/PDADMAC
TS (g/L)	16.7
water content removal (g-H_2O/g-DS)	148.5
water content of WAS cake (%)	66.1
amount of WAS (dry tonne/year)	1000
ferrous sulfate ($/year)	75,000
sodium persulfate ($/year)	7000
zeolites ($/year)	6000
PDADMAC ($/year)	120,000
total cost ($/dry tonne)	208
total cost ($/year)	208,000

[a]For the Fe(II)/$S_2O_8^{2-}$/zeolites/PDADMAC process, the dosages of Fe(II), $S_2O_8^{2-}$, zeolites, and PDADMAC were 2.25 and 1.8 mmol/g-VS, 0.5 g/g-VS, and 0.3 g/g-VS, respectively. The price of ferrous sulfate, potassium persulfate, zeolites, and PDADMAC are $60, $25, $30, and $1000/tonne, respectively.

in cells, and flocs were released into the liquid phase. When the WAS was pretreated by Fe(II)/$S_2O_8^{2-}$ combined with 0.5 g-zeolites/g-VS, an additional decrease of 0.06 g-BW/g-DS occurred. The multiple void skeletal lattice of zeolites, which might have impeded the stacking of particles, offered the channel and pathway for bounded water escape. On the other hand, zeolites prevented the pores on filter cloth from clogging and subsequently accelerated the water filtration rate.

Furthermore, at the optimal conditions of 2.25/1.8 mmol-Fe(II)/$S_2O_8^{2-}$/g-VS, 0.5 g-zeolites/g-VS, and 0.3 g-PDADMAC/g-VS, TW and FW contents were decreased by 74 and 83.4% compared with the raw WAS, respectively. The bound water escaped via the channels, and the hydrophilic flocs were absorbed by PDADMAC molecules. Therefore, the water removal efficiency was further enhanced greatly. Note that BW content of the WAS cake showed a slight increase (i.e., 0.42 g/g-DS) compared with that of the combined Fe(II)/$S_2O_8^{2-}$ and zeolites. This might be due to the fact that long loops and tails extended and intertwined each other[38] caused by electrostatic repulsion.[39] As a result, part of the released water was recaptured and bounded. However, the FW and TW were 1.16 and 0.74 g/g-DS lower, respectively, indicating the importance of PDADMAC in the advanced dewatering of WAS. In sharp contrast, the single usage of PDADMAC, similar to the commonly used inorganic or organic flocculants (e.g., iron or aluminum salts),[41,42] could hardly disintegrate the EPS structure and convert bound water into free water and in some cases even deteriorate the dewatering efficiency. Differently, PDADMAC, as one kind of polyelectrolyte with high molecular weight and low charge density,[42] could play a positive part in the solid−water separation and dewatering[40−42] when combined with Fe(II)/$S_2O_8^{2-}$ oxidation as proven in the current study, mainly because of its reflocculation effect on the broken WAS flocs by Fe(II)/$S_2O_8^{2-}$ oxidation.[43,44] Those observations provided a solid proof of the occurrence of the synergistic effect of PDADMAC with Fe(II)/$S_2O_8^{2-}$ and zeolites as well as its critical role in promoting water liberation.

Variations in Composition of Different EPS Fractions. Extracellular polymeric substances (EPSs), consisting mostly of protein (PN) and polysaccharide (PS), are regarded as one of the most important factors that influence the dewaterability.[45] As illustrated in Figure 4a, Fe(II)/$S_2O_8^{2-}$ pretreatment had a profound effect on the distribution of EPS. Total EPS (PN + PS) in the S-EPS fraction increased gradually with increasing Fe(II)/$S_2O_8^{2-}$ dosage, whereas the content of LB-EPS and TB-EPS decreased slightly. Total EPSs in S-EPS, LB-EPS, and TB-EPS fractions in raw WAS were 9.9, 13.2, and 46.3 mg/g-VS, respectively. When Fe(II)/$S_2O_8^{2-}$ dosage was increased to 3.75/3 mmol/g-VS, the EPS content in the S-EPS fraction increased to 29.4 mg/g-VS, whereas LB-EPS and TB-EPS decreased to 8.9 and 36.0 mg/g-VS, respectively. The result showed that not merely were LB-EPS and TB-EPS fractions shifted to the S-EPS fraction, but also part of S-EPS was degraded. Fe(II)/$S_2O_8^{2-}$, as a strong oxidation agent, has changed the distribution of different EPS fractions while simultaneously degrading the soluble organics. This finding is an agreement with the previous works of Zhen et al.[9,13] When conditioned with fixed Fe(II)/$S_2O_8^{2-}$ dosage (2.25/1.8 mmol/g-VS), EPS fractions showed a slight decrease when the zeolite

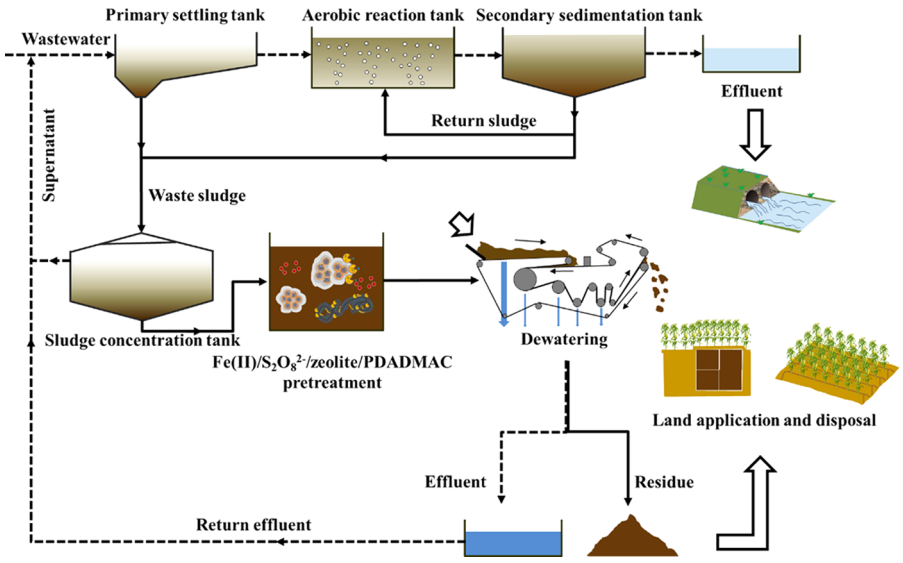

Figure 9. Technological process flowchart of the WAS processing steps via Fe(II)/$S_2O_8^{2-}$/zeolites/PDADMAC.

DOI: 10.1021/acssuschemeng.9b03842
ACS Sustainable Chem. Eng. 2019, 7, 16549−16559

dosage was elevated from 0 to 0.5 g/g-VS. There occurred a mild ascend in LB-EPS and TB-EPS fractions by 18 and 16.2%, respectively, when the zeolite dosage was increased to 0.8 g/g-VS. This is mainly due to the fact that zeolites have a rough and porous structure with defined channels/cavities and that they can offer more ultravast space and sites for $SO_4\cdot^-$ generation and chemical transformation. As a result, more intracellular substances were released. It should be noted that superfluous zeolites led to the incarceration of $SO_4\cdot^-$ inside the cages through unfavorable Coulomb interactions with the zeolite framework.[46] In this regard, the number of available $SO_4\cdot^-$ decreased compared with other conditions, which subsequently exhibited less powerful destruction to EPS. Besides, zeolites played a supportive role in water release during the filtration as it prevented filtration pores from being plugged with small particles from the decomposition of WAS flocs caused by Fe(II)/$S_2O_8^{2-}$. In general, the conditioning with 2.25/1.8 mmol-Fe(II)/$S_2O_8^{2-}$/g-VS and 0.5 g-zeolites/g-VS performed better than those with higher dosage of zeolites.

As expected, the further addition of PDADMAC gave rise to more obvious variations in the distribution of EPS fractions (Figure 4c). At a fixed Fe(II)/$S_2O_8^{2-}$ and zeolite dosages (2.25/1.8 mmol/g-VS and 0.5 g/g-VS), a merger decline in LB-EPS and TB-EPS was noticed when PDADMAC dosage was increased to 0.3 g/g-VS, that is, 77.0 and 35.4% decrease, respectively. Contrarily, they reclimbed by 146.1 and 3.9% when further increasing PDADMAC to 0.8 g/g-VS. In contrast, no significant variation in S-EPS was noticed under the all conditions, reflecting that the PDADMAC had mainly affected LB-EPS and TB-EPS fractions rather than S-EPS. At an appropriate dosage, PDADMAC could flocculate the WAS and small particles via electrical neutralization and adsorption bridging, accelerating the solid sedimentation. Note that at excess PDADMAC dosage, the negative charges located on the surface of WAS particles were completely neutralized and then quickly charged with positive electric charges. The positively charged WAS particles tended to be resuspended due to high internal charge repulsion, causing a high osmotic swelling pressure and increased water retention,[42] thus resulting in the deteriorated dewaterability.

EPS has a high affinity for water and is highly hydrated with water content up to 98%,[47] and thus, the WAS with high-content EPS is more difficult to dewater. Due to the discrepancy in spatial distribution of WAS flocs, each kind of EPS plays a different role in the dewatering process. S-EPSs diffuse in the liquid phase of WAS, and the water around S-EPS can be easily separated via filtration. As a result, the S-EPS fraction could barely have influence on WAS dewaterability.[13] By contrary, LB-EPS and TB-EPS are regarded as the key factors affecting dewaterability. LB-EPS, located in the space between the surface of WAS flocs and the liquid phase, is highly dispersive and porous.[32] A previous study by Yu et al.[48] verified the strongly positive correlation between LB-EPS and WAS dewatering performance because of the large water retention capability of LB-EPS. The excessive LB-EPS may retain higher EPS-binding water,[9,49] which results in poor dewaterability. Thus, the degradation of LB-EPS could reduce the water binding energy, leading to the increase in WAS dewatering. TB-EPSs, tightly attached onto the surface of cells as a shield, restrict the lysis of cells and thus the release of intracellular water and substances, in consensus with Lee et al.[50] Hence, the degradation of LB-EPS and TB-EPS caused by Fe(II)/$S_2O_8^{2-}$/zeolites/PDADMAC pretreatment is the key cause of the promoted dewaterability.

Distribution of Key Organic Components in the WAS Flocs. The confocal laser scanning microscopy (CLSM) technique is able to visualize the horizontal distribution of bacteria cells and biopolymers[51] and the spatial structure of WAS flocs via 2D merging and 3D merging graphs. By staining different colors, protein, α-polysaccharide, lipid, dead cells, and living cells can be identified vividly.

Protein (green), α-polysaccharide (blue), and living cells (cyan) were detected in a highly nonuniform manner (Figure 5a), reflecting that the raw WAS flocs mainly exist in the form of bulks, with water bounded inside as well as living cells and few dead cells observed. The biopolymers and cells coexisted to form the complex zoogloeal matrix. After conditioned with Fe(II)/$S_2O_8^{2-}$, the colors represented by protein, α-polysaccharide, and living cells faded (Figure 5b). It revealed that Fe(II)/$S_2O_8^{2-}$ oxidation caused the rupture and lysis of living and dead cells, with plenty of biopolymers (i.e., protein and α-polysaccharide), and EPS- and cell-bound water released into the liquid phase in conformity with the results of LB-EPS and TB-EPS given in Figure 4a. Due to the low content of lipid, nearly no change was found in this component. It is worth noting that further addition of zeolites changed the distribution of the components also. As shown in Figure 5b, all the colors became stronger and distributed more uniformly with a large amount of tiny vacancy inside created by zeolites. The tiny vacancy acted as the channel and passage, facilitating bound water liberation during the filtration phase, correlating well with the observations obtained in Dewatering Performance via Single or Zeolites and Dewatering Performance via the Combined Process sections. When conditioned with Fe(II)/$S_2O_8^{2-}$, zeolites and PDADMAC, the distribution of the colors became much more concentrated, especially green and blue, indicating the aggregation of protein, α-polysaccharide, and living cells (Figure 5a,d). At the same time, different colors in the merging graph (Figure 5d) showed highly uniform overlap. It reveals that all the hydrophilic particles originated from the rupture of flocs and cells were reflocculated by electrical neutralization and adsorption bridging of PDADMAC, as a result of which, WAS dewaterability was promoted profoundly.

Decisive Composition and Structure Linked to WAS Dewaterability. XPS measurements were utilized to reveal the chemical change of C, N, O, and Si elements in the WAS before and after pretreatment. High-resolution XPS spectra at C 1s show the appearance of four main C-containing species (Figure 6). The typical peaks at 284.5 and 286.1 eV were assigned to aliphatic/aromatic carbon (C−C, C−H, and C═C)[52] and carbon bounded as C−O and C−N (amide I), respectively.[53] The peak at 287.5 eV corresponded to the O═C—NH− bond of amino acid,[52] which was also recognized in the O 1s high-resolution spectrum (the peak at 532.3 eV) and the N 1s high-resolution region (the peaks at 399.6 and 400.8 eV). The peak at 288.5 eV was related to the O—C═O bond of the carboxyl acids. The peaks at 530.8 and 531.5 eV were assigned to O−H and C═O, respectively. The peaks at 530.8 and 531.5 eV were linked to oxygen bounded as O−H, and C═O.[53,54] The peaks at 102.2 and 101.8 were characteristics of Si−O−Si−O and SiO_2, and the peaks located at 103.2 corresponded to Almand. The peaks, which was related to O−H and C−O, the two most common functional groups in carbohydrate,[55] revealed the presence of polysaccharide while the peaks linked to C−C, C−H, C−N, C═O, and O═C—

DOI: 10.1021/acssuschemeng.9b03842
ACS Sustainable Chem. Eng. 2019, 7, 16549−16559

NH− reflected the presence of protein. The high relative intensities in raw WAS meant high content of PN and PS before the pretreatment. The peaks indicated by Si−O−Si−O and SiO_2 provided the direct evidence for the existence of zeolites. High peaks related to those elements reflected the presence of a high-content silicon compound in conformity with the finding of Dai et al.[52] In sharp contrast, the corresponding intensities of peaks related to C−C, O═C—NH−, and O−H decreased to some extent after Fe(II)/$S_2O_8^{2-}$ oxidation. When combining Fe(II)/$S_2O_8^{2-}$ and zeolites, the intensities of peaks related to O═C—NH− and O−H decreased more obviously, indicating the decomposition of PN-like and PS-like substances caused by the strong Fe(II)/$S_2O_8^{2-}$ oxidation, in accordance with the EPS results (Figure 4). Meanwhile, the intensity of peaks related to Si−O−Si−O and SiO climbed dramatically, attributed to the addition of zeolites with silica tetrahedron (SiO_4) as the main component.[20] As expected, the intensities of peaks related to O═C—NH−, C−C, and Si−O−Si−O kept nearly unchanged in the presence of PDADMAC, presumably due to the lack of the capability of rupturing the flocs or degrading biopolymers. It is commonly accepted that the water binding properties depend mainly on the interactions of the biopolymers (including PN and PS) with the hydrogen bond. Fe(II)/$S_2O_8^{2-}$ oxidation causes the rupture of the related bond, the disintegration of biopolymers, and the release of water. Moreover, the addition of zeolites and PDADMAC is able to further reduce the water binding energy through providing channel/cages or reflocculating hydrophilic particles. As a consequence, WAS dewaterability was strengthened greatly.

Change of the Microstructure of WAS Flocs by SEM-EDS Observation. To reveal the underlying mechanism of dewatering, the microstructure of WAS was observed via SEM-EDS analysis (Figure 7). The raw WAS existed in the shape of *Zoogloea* with a large number of intact microbial cells colonizing in microcolonies and gel-like EPS filling the space among the microcolonies (Figure 7a). The aggregates interlaced with each other closely, forming a glutinous and pilotaxitic structure, with water and biopolymers (see carbon and oxygen EDS mapping in Figure 7a) bound inside, which resulted in poor dewaterability, matching well with the finding from Zhang et al.[5] Comparatively, an apparent change in morphology was identified when conditioned with Fe(II)/$S_2O_8^{2-}$ (Figure 7b). When exposed to Fe(II)/$S_2O_8^{2-}$ oxidation, the EPSs located in the out layer of WAS flocs were damaged initially and the cell walls without the protective layer tended to be broken down more easily. Hence, plenty of intracellular water was released into the liquid phase through the crack of cells.

Further addition of zeolites created more tiny channels/cavities in the WAS flocs, as observed in Figure 7c. Owing to the multiple void skeletal lattice, the needful energy for water and biopolymer removal from WAS flocs decreased. As a result, the bound water could be released easily. The observations consisted with the results in EPS analysis (Change in Water Distribution of WAS Flocs section) and CLSM observation (Distribution of Key Organic Components in the WAS Flocs section). When subjected to Fe(II)/$S_2O_8^{2-}$, zeolites, and PDADMAC, the WAS flocs became much more bulky and flocculent as expected (Figure 7d), owing to the long chain of PDADMAC. Compared with the raw WAS, the cells were totally damaged under Fe(II)/$S_2O_8^{2-}$ oxidation, and the WAS flocs were broken into small particles with bound water release. However, PDADMAC reflocculated the particles including some hydrophilic groups, forming larger porous floccules. As expressed by EDS mapping, the distribution of carbon, oxygen, and nitrogen became more even at first and then decreased rapidly, unravelling that most of the WAS flocs and the constituents included were disrupted by Fe(II)/$S_2O_8^{2-}$ oxidation. As a function of the finding above, the underlying mechanism of dewatering could be concluded as three steps: (i) the $SO_4^{\cdot-}$ generated by Fe(II)/$S_2O_8^{2-}$ oxidation attacked the WAS flocs and cells, broke the bonds of O−H, C−C, and O═C—NH− in high-molecular-weight biopolymers, and further decomposed them into micromolecule organics and even inorganics, thus liberating EPS- and cell-bound water, (ii) the broken WAS flocs were then reflocculated via adsorption bridging and charge neutralization induced by PDADMAC, and (iii) during the subsequent filtration, zeolites created channels/cavities for water release by forming a multiple void skeletal lattice while alleviating the clogging of filtration cloth. For the better visualization of the synergistic effect of Fe(II) persulfate oxidation coupled with zeolites and PDADMAC for positive feedbacks to WAS dewaterability, the possible catalyzing behaviors and dewatering principles are illustrated in Figure 8.

Economic Analysis. The cost of WAS management takes up about 50% of the total operating cost of the wastewater treatment plant;[56] hence, it is vital to take a cost-benefit analysis to evaluate the economic feasibility of the WAS process before practice. To explore the practice potential of the Fe(II)/$S_2O_8^{2-}$/zeolites/PDADMAC process, a desktop scalingup cost-benefit analysis was carried out based on a WWTP with a population equivalent of 100,000. The optimal condition for WAS dewatering obtained in the current study was applied in this scenario. According to Table 3, the whole pretreatment process costed $208,000 per year, saving up to 45.6% (382,400 per year) and 61.3% (538,000 per year) compared with some representative methods such as the ZVI/persulfate and classical Fenton process.[57] More importantly, the current process performed better than the ZVI/persulfate or classical Fenton process in sludge dewatering. Based on the results, a potential technological process for using Fe(II)/$S_2O_8^{2-}$/zeolites/PDADMAC to enhance WAS dewaterability in a WWTP is proposed (Figure 9). It should be noted that for an accurate calculation, the present worth, equivalent annual worth, and market for renewable energy exchange also, all should be considered, in addition to the cost for conditioning chemicals. Besides, the local circumstance of labor, the maintenance frequency of devices, the cost for mechanical dewatering transportation and final disposal (e.g., land application, incineration, landfill, etc.) should also be included. More importantly, the evaluation results might vary greatly with the operation skill of operator, land price, and discharge standards in the real-world scenarios.[58] Thus, full-scale investigation is still needed to evaluate the economic and environmental benefits of the Fe(II)/$S_2O_8^{2-}$/zeolites/PDADMAC process more legitimately.

■ CONCLUSIONS

This study demonstrated that the combination of Fe(II)/$S_2O_8^{2-}$, zeolites, and PDADMAC had a significant effect on enhancing WAS dewaterability and the optimal conditions obtained were 2.25/1.8 mmol-Fe(II)/$S_2O_8^{2-}$/g-VS, 0.5 g-zeolites/g-VS, and 0.3 g-PDADMAC/g-VS with up to 117 g-H_2O/g-VS removal (moisture content: 64.5%). Further

DOI: 10.1021/acssuschemeng.9b03842
ACS Sustainable Chem. Eng. 2019, 7, 16549−16559

analysis revealed the three-step dewatering mechanisms: (i) the $SO_4^{\cdot -}$ generated by Fe(II)/$S_2O_8^{2-}$ oxidation attacked the WAS flocs and cells, broke the bonds of O−H, C−C, and O═C—NH− in high-molecular-weight biopolymers, and further decomposed them into micromolecule organics and even inorganics, thus liberating EPS- and cell-bound water, (ii) the broken WAS flocs were then reflocculated via adsorption bridging and charge neutralization induced by PDADMAC, and (iii) during the subsequent filtration, zeolites created channels/cavities for water release by forming a multiple void skeletal lattice while alleviating the clogging of filtration cloth. Furthermore, the pretreatment of the Fe(II)/$S_2O_8^{2-}$/zeolites/PDADMAC process costed $208,000 per year, saving up to 45.6% (382,400 per year) and 61.3% (538,000 per year) compared with the ZVI/persulfate and classical Fenton process, which represent the enormous potential in practices.

■ ASSOCIATED CONTENT

Supporting Information

The Supporting Information is available free of charge on the ACS Publications website at DOI: 10.1021/acssuschemeng.9b03842.

Pretreatment by Fe(II)/$S_2O_8^{2-}$ oxidation; addition of zeolites as skeleton builder; Fe(II)/$S_2O_8^{2-}$ with zeolites as skeleton builder; performance of integrated Fe(II)/$S_2O_8^{2-}$-zeolites-PDADMAC process (PDF)

■ AUTHOR INFORMATION

Corresponding Authors

*E-mail: gyzhen@des.ecnu.edu.cn. Phone: 86-21-5434-1145.
*E-mail: xqlu@des.ecnu.edu.cn. Phone: 86-021-33503245.

ORCID

Guangyin Zhen: 0000-0003-4747-3027

Notes

The authors declare no competing financial interest.

■ ACKNOWLEDGMENTS

This work was sponsored by the Science & Technology Innovation Action Plan of Shanghai under the Belt and Road Initiative (no. 17230741100), the Distinguished Professor in Universities of Shanghai (Oriental Scholar, no. TP2017041), the Shanghai Pujiang Program (no. 17PJ1402100), the Fundamental Research Funds for the Central Universities, the Shanghai Yangfan Program (no. 19YF1414000), and the Shanghai Institute of Pollution Control and Ecological Security.

■ REFERENCES

(1) Yang, C.; Meng, X. Z.; Chen, L.; Xia, S. Polybrominated diphenyl ethers in sewage sludge from Shanghai, China: possible ecological risk applied to agricultural land. *Chemosphere* **2011**, *85*, 418−423.

(2) Guo, X.; Wang, Y.; Wang, D. Permanganate/bisulfite (PM/BS) conditioning-horizontal electro-dewatering (HED) of activated sludge: Effect of reactive Mn(III) species. *Water Res.* **2017**, *124*, 584−594.

(3) Raynaud, M.; Vaxelaire, J.; Olivier, J.; Dieudé-Fauvel, E.; Baudez, J. C. Compression dewatering of municipal activated sludge: effects of salt and pH. *Water Res.* **2012**, *46*, 4448−4456.

(4) Mahmoud, A.; Olivier, J.; Vaxelaire, J.; Hoadley, A. F. Electrical field: a historical review of its application and contributions in wastewater sludge dewatering. *Water Res.* **2010**, *44*, 2381−2407.

(5) Zhang, J.; Yang, K.; Wang, H.; Zheng, L.; Ma, F.; Lv, B. Impact of microwave treatment on dewaterability of sludge during Fenton oxidation. *Desalin. Water Treat.* **2015**, *57*, 14424−14432.

(6) Devlin, D. C.; Esteves, S. R. R.; Dinsdale, R. M.; Guwy, A. J. The effect of acid pretreatment on the anaerobic digestion and dewatering of waste activated sludge. *Bioresour. Technol.* **2011**, *102*, 4076−4082.

(7) Feng, X.; Deng, J.; Lei, H.; Bai, T.; Fan, Q.; Li, Z. Dewaterability of waste activated sludge with ultrasound conditioning. *Bioresour. Technol.* **2009**, *100*, 1074−1081.

(8) Moreira, F. C.; Soler, J.; Fonseca, A.; Saraiva, I.; Boaventura, R. A.; Brillas, E.; Vilar, V. J. Electrochemical advanced oxidation processes for sanitary landfill leachate remediation: Evaluation of operational variables. *Appl. Catal., B* **2016**, *182*, 161−171.

(9) Zhen, G. Y.; Lu, X. Q.; Zhao, Y. C.; Chai, X. L.; Niu, D. J. Enhanced dewaterability of sewage sludge in the presence of Fe(II)-activated persulfate oxidation. *Bioresour. Technol.* **2012**, *116*, 259−265.

(10) Zhen, G.; Lu, X.; Wang, B.; Zhao, Y.; Chai, X.; Niu, D.; Zhao, A.; Li, Y.; Song, Y.; Cao, X. Synergetic pretreatment of waste activated sludge by Fe(II)-activated persulfate oxidation under mild temperature for enhanced dewaterability. *Bioresour. Technol.* **2012**, *124*, 29−36.

(11) Zhen, G.; Wang, J.; Lu, X.; Su, L.; Zhu, X.; Zhou, T.; Zhao, Y. Effective gel-like floc matrix destruction and water seepage for enhancing waste activated sludge dewaterability under hybrid microwave-initiated Fe(II)-persulfate oxidation process. *Chemosphere* **2019**, *221*, 141−153.

(12) Wu, C.; Jin, L.; Zhang, P.; Zhang, G. Effects of potassium ferrate oxidation on sludge disintegration, dewaterability and anaerobic biodegradation. *Int. Biodeterior. Biodegrad.* **2015**, *102*, 137−142.

(13) Zhen, G. Y.; Lu, X. Q.; Li, Y. Y.; Zhao, Y. C. Innovative combination of electrolysis and Fe(II)-activated persulfate oxidation for improving the dewaterability of waste activated sludge. *Bioresour. Technol.* **2013**, *136*, 654−663.

(14) Khosravi, A.; Esmhosseini, M.; Jalili, J.; Khezri, S. Optimization of ammonium removal from waste water by natural zeolite using central composite design approach. *J. Inclusion Phenom. Macrocyclic Chem.* **2012**, *74*, 383−390.

(15) He, D. Q.; Luo, H. W.; Huang, B. C.; Qian, C.; Yu, H. Q. Enhanced dewatering of excess activated sludge through decomposing its extracellular polymeric substances by a Fe@Fe_2O_3-based composite conditioner. *Bioresour. Technol.* **2016**, *218*, 526−532.

(16) Shi, H.; Zhu, J.; Chen, J.; Qiu, X. In Experiment Study on the effects of natural zeolite on sludge dewatering performance and nitrogen losses, *International Conference on Material and Environmental Engineering (ICMAEE 2014)*; Atlantis Press: Paris, 2014.

(17) Benítez, J.; Rodríguez, A.; Suárez, A. Optimization technique for sewage sludge conditioning with polymer and skeleton builders. *Water Res.* **1994**, *28*, 2067−2073.

(18) Weckhuysen, B. M.; Yu, J. Recent advances in zeolite chemistry and catalysis. *Chem. Soc. Rev.* **2015**, *44*, 7022−7024.

(19) Moliner, M.; Martinez, C.; Corma, A. Multipore zeolites: synthesis and catalytic applications. *Angew. Chem., Int. Ed.* **2015**, *54*, 3560−3579.

(20) Weitkamp, J. Zeolites and catalysis. *Solid State Ionics* **2000**, *131*, 175−188.

(21) Mohseni-Bandpi, A.; Al-Musawi, T. J.; Ghahramani, E.; Zarrabi, M.; Mohebi, S.; Vahed, S. A. Improvement of zeolite adsorption capacity for cephalexin by coating with magnetic Fe_3O_4 nanoparticles. *J. Mol. Liq.* **2016**, *218*, 615−624.

(22) Kim, J.-O.; Kim, S.; Park, N.-S. Performance and modeling of zeolite adsorption for ammonia nitrogen removal. *Desalin. Water Treat.* **2012**, *43*, 113−117.

(23) Zhang, R.; Liu, N.; Lei, Z.; Chen, B. Selective Transformation of Various Nitrogen-Containing Exhaust Gases toward N_2 over Zeolite Catalysts. *Chem. Rev.* **2016**, *116*, 3658−3721.

DOI: 10.1021/acssuschemeng.9b03842
ACS Sustainable Chem. Eng. 2019, 7, 16549−16559

(24) Shen, C.; Ma, J.; Liu, W.; Wen, Y.; Rashid, S. Selective conversion of organic pollutant p-chlorophenol to formic acid using zeolite Fenton catalyst. *Chemosphere* **2016**, *161*, 446−453.
(25) Lee, D. J.; Lee, S. F. Measurement of bound water content in sludge: The use of differential scanning calorimetry (DSC). *J. Chem. Technol. Biot.* **1995**, *62*, 359−365.
(26) Walter, W. G. Standard methods for the examination of water and wastewater (11th ed.). *Am. J. Publ. Health Nations Health* **1961**, *51*, 940.
(27) Feng, J.; Wang, Y. L.; Ji, X. Y. Dynamic changes in the characteristics and components of activated sludge and filtrate during the pressurized electro-osmotic dewatering process. *Sep. Purif. Technol.* **2014**, *134*, 1−11.
(28) Zhang, Z.; Song, Y.; Zheng, S.; Zhen, G.; Lu, X.; Kobayashi, T.; Xu, K.; Bakonyi, P. Electro-conversion of carbon dioxide (CO_2) to low-carbon methane by bioelectromethanogenesis process in microbial electrolysis cells: The current status and future perspective. *Bioresour. Technol.* **2019**, *279*, 339−349.
(29) APHA. *Standard Methods for the Examination of Water and Wastewater*, 20th ed.; A.P.H. Association: Washington, DC, 1998.
(30) Dubois, M.; Giles, K.; Rebers, P.; Smith, F. Colorimetric method for determination of Sugars and related substances. *Anal. Chem.* **1956**, *28*, 350−356.
(31) Frølund, B.; Palmgren, R.; Keiding, K.; Nielsen, P. Extraction of Extracellular Polymers from Activated Sludge Using a Cation Exchange Resin. *Water Res.* **1996**, *30*, 1749−1758.
(32) Zhen, G.; Lu, X.; Su, L.; Kobayashi, T.; Kumar, G.; Zhou, T.; Xu, K.; Li, Y. Y.; Zhu, X.; Zhao, Y. Unraveling the catalyzing behaviors of different iron species (Fe2+ vs. Fe0) in activating persulfate-based oxidation process with implications to waste activated sludge dewaterability. *Water Res.* **2018**, *134*, 101−114.
(33) Liu, H.; Yang, J. K.; Zhu, N. R.; Zhang, H.; Li, Y.; He, S.; Yang, C. Z.; Yao, H. A comprehensive insight into the combined effects of Fenton's reagent and skeleton builders on sludge deep dewatering performance. *J. Hazard. Mater.* **2013**, *258*, 144−150.
(34) Lee, C. H.; Liu, J. C. Enhanced Sludge Dewatering by Dual Polyelectrolytes Conditioning. *Water Res.* **2000**, *34*, 4430−4436.
(35) He, D. Q.; Wang, L. F.; Jiang, H.; Yu, H. Q. A Fenton-like process for the enhanced activated sludge dewatering. *Chem. Eng. J.* **2015**, *272*, 128−134.
(36) Zhou, X.; Wang, Q.; Jiang, G.; Zhang, X.; Yuan, Z. Enhancing dewaterability of waste activated sludge by combined oxidative conditioning process with zero-valent iron and peroxymonosulfate. *Water Sci. Technol.* **2017**, *76*, 2427−2433.
(37) Wang, Q.; Wei, W.; Liu, S.; Yan, M.; Song, K.; Mai, J.; Sun, J.; Ni, B.; Gong, Y. Free Ammonia Pretreatment Improves Degradation of Secondary Sludge During Aerobic Digestion. *ACS Sustainable Chem. Eng.* **2017**, *6*, 1105.
(38) Lee, C. S.; Robinson, J.; Chong, M. F. A review on application of flocculants in wastewater treatment. *Process Saf. Environ. Prot.* **2014**, *92*, 489−508.
(39) Caskey, J. A.; Primus, R. J. The effect of anionic polyacrylamide molecular conformation and configuration on flocculation effectiveness. *Environ. Prog.* **1986**, *5*, 98−103.
(40) Niu, M.; Zhang, W.; Wang, D.; Chen, Y.; Chen, R. Correlation of physicochemical properties and sludge dewaterability under chemical conditioning using inorganic coagulants. *Bioresour. Technol.* **2013**, *144*, 337−343.
(41) Zhang, W.; Chen, Z.; Cao, B.; Du, Y.; Wang, C.; Wang, D.; Ma, T.; Xia, H. Improvement of wastewater sludge dewatering performance using titanium salt coagulants (TSCs) in combination with magnetic nano-particles: Significance of titanium speciation. *Water Res.* **2017**, *110*, 102−111.
(42) Saveyn, H.; Meersseman, S.; Thas, O.; Van der Meeren, P. Influence of polyelectrolyte characteristics on pressure-driven activated sludge dewatering. *Colloids Surf., A* **2005**, *262*, 40−51.
(43) Thapa, K. B.; Qi, Y.; Hoadley, A. F. A. Interaction of polyelectrolyte with digested sewage sludge and lignite in sludge dewatering. *Colloids Surf., A* **2009**, *334*, 66−73.
(44) Mohammad, T .A.; Mohamed, E. H.; Noor, M. J. M. M.; Ghazali, A. H. Dual polyelectrolytes incorporatingMoringa oleiferain the dewatering of sewage sludge. *Desalin. Water Treat.* **2014**, *55*, 3613−3620.
(45) Zhen, G.; Lu, X.; Li, Y.; Zhao, Y.; Wang, B.; Song, Y.; Chai, X.; Niu, D.; Cao, X. Novel insights into enhanced dewaterability of waste activated sludge by Fe(II)-activated persulfate oxidation. *Bioresour. Technol.* **2012**, *119*, 7−14.
(46) Hermenegildo, G.; Roth, H. D. Generation and reactions of organic radical cations in zeolites. *Chem. Rev.* **2002**, *102*, 3947−4008.
(47) Jin, B.; Wilén, B.-M.; Lant, P. Impacts of morphological, physical and chemical properties of sludge flocs on dewaterability of activated sludge. *Chem. Eng. J.* **2004**, *98*, 115−126.
(48) Yu, W.; Yang, J.; Tao, S.; Shi, Y.; Yu, J.; Lv, Y.; Liang, S.; Xiao, K.; Liu, B.; Hou, H.; Hu, J.; Wu, X. A comparatively optimization of dosages of oxidation agents based on volatile solids and dry solids content in dewatering of sewage sludge. *Water Res.* **2017**, *126*, 342−350.
(49) Li, X. Y.; Yang, S. F. Influence of loosely bound extracellular polymeric substances (EPS) on the flocculation, sedimentation and dewaterability of activated sludge. *Water Res.* **2007**, *41*, 1022−1030.
(50) Lee, K. M.; Kim, M. S.; Lee, C. Oxidative treatment of waste activated sludge by different activated persulfate systems for enhancing sludge dewaterability. *Sustainable Environ. Res.* **2016**, *26*, 177−183.
(51) Meng, F.; Yang, F. Fouling mechanisms of deflocculated sludge, normal sludge, and bulking sludge in membrane bioreactor. *J. Membr. Sci.* **2007**, *305*, 48−56.
(52) Dai, X.; Xu, Y.; Dong, B. Effect of the micron-sized silica particles (MSSP) on biogas conversion of sewage sludge. *Water Res.* **2017**, *115*, 220−228.
(53) Castillo, G. A.; Wilson, L.; Efimenko, K.; Dickey, M. D.; Gorman, C. B.; Genzer, J. Amidation of Polyesters Is Slow in Nonaqueous Solvents: Efficient Amidation of Poly(ethylene terephthalate) with 3-Aminopropyltriethoxysilane in Water for Generating Multifunctional Surfaces. *ACS Appl. Mater. Interfaces* **2016**, *8*, 35641−35649.
(54) Wen, Z.; Zhang, Y.; Dai, C. Removal of phosphate from aqueous solution using nanoscale zerovalent iron (nZVI). *Colloids Surf., A* **2014**, *457*, 433−440.
(55) Mecozzi, M.; Pietrantonio, E. Carbohydrates proteins and lipids in fulvic and humic acids of sediments and its relationships with mucilaginous aggregates in the Italian seas. *Mar. Chem.* **2006**, *101*, 27−39.
(56) Dhar, B. R.; Nakhla, G.; Ray, M. B. Techno-economic evaluation of ultrasound and thermal pretreatments for enhanced anaerobic digestion of municipal waste activated sludge. *Waste Manage.* **2012**, *32*, 542−549.
(57) Zhou, X.; Wang, Q. L.; Jiang, G. M.; Liu, P.; Yuan, Z. G. A novel conditioning process for enhancing dewaterability of waste activated sludge by combination of zero-valent iron and persulfate. *Bioresour. Technol.* **2015**, *185*, 416−420.
(58) Zhen, G.; Lu, X.; Kato, H.; Zhao, Y.; Li, Y. Overview of pretreatment strategies for enhancing sewage sludge disintegration and subsequent anaerobic digestion: Current advances, full-scale application and future perspectives. *Renewable Sustainable Energy Rev.* **2017**, *69*, 559−577.

DOI: 10.1021/acssuschemeng.9b03842
ACS Sustainable Chem. Eng. 2019, 7, 16549−16559